Progress In Electromagnetics Research C, Vol. 118, 247–262, 2022

Compact MIMO Antenna Designs Based on Hybrid Fractal Geometry for 5G Smartphone Applications

Muhannad Y. Muhsin*, Ali J. Salim, and Jawad K. Ali

Abstract—Compact low-profile four and eight elements Multi-Input Multi-Output (MIMO) antenna arrays are presented for 5G smartphone devices. The proposed antenna systems can operate at two wide bands with triple resonance frequencies that cover the extended Personal Communication Purposes (PCS) n25 band and other related applications, the mobile china's band, and the LTE Band-46. The proposed antenna element is designed based on modified Minkowski and Peano curves fractal geometries. Desirable antenna miniaturization with multi-band capability is obtained by utilizing the space-filling and self-similarity properties of the proposed hybrid fractal geometries where the overall antenna size is (11.47 mm × 7.19 mm). All antennas are printed on the surface layer of the main mobile board. Based on the self-isolated property, good isolation is attained without employing additional decoupling structures and/or isolation techniques, increasing system complexity and reducing antenna efficiency. For evaluating the performance of the proposed antenna systems, the scattering parameters, antenna efficiencies, antenna gains, antenna radiation characteristics, envelope correlation coefficients (ECCs), and mean effective gains (MEGs) are investigated. The performances are evaluated to confirm the suitability of the proposed MIMO antenna systems for 5G mobile terminals. The proposed eight elements MIMO system has been fabricated and tested. The measured and simulated results are in good agreement.

1. INTRODUCTION

With the increasing growth of wireless communication technologies, high data rates and intelligent services are continuously demanded. Because of the advantages of large channel capacity, massive connection density, and high spectral efficiency, the 5G wireless communication systems have attracted increasing attention in academic and industrial fields [1]. One of the essential enabling technologies for the 5G communication systems is the Multiple Input Multiple Output (MIMO) technology. By utilizing the multipath property of the wireless communication environment, a MIMO system can improve the spectral efficiency and channel capacity without needing more bandwidth and/or transmitting power [2]. Increasing the MIMO system's antenna elements allows for larger channel capacity and more link reliability [3–5]. However, because of mobile devices' limited space, the mutual coupling problem is becoming more pronounced with more penetration of antennas. The mutual coupling impact severely affects the MIMO system's performance [6]. So, various techniques have been employed and provided reasonable solutions to solve this problem. One of these techniques is the spatial diversity method [7–9]. Good isolation can be obtained by this method but at the expense of decreasing the number of antennas, where the space variation between antennas is used as a key approach to achieving low mutual coupling. Isolation enhancement can be done with more compactness than the spatial diversity method by employing the polarization diversity method [10, 11] and the pattern diversity method [12, 13]. However, the compact size and simple structure design of 5G mobile devices, which

Received 28 January 2022, Accepted 23 February 2022, Scheduled 3 March 2022
* Corresponding author: Muhannad Y. Muhsin (muhannad.y.muhsin@uotechnology.edu.iq).
The authors are with the Microwave Research Group, Department of Electrical Engineering, University of Technology, Iraq.

have high diversity performance capability with low ECCs, remains a highly requested aim for antenna engineers in designing MIMO antenna systems. Moreover, many other isolation techniques using external decoupling structures have been reported in the literature. These techniques include parasitic structure [14, 15], hybrid elements (neutralization line and parasitic element) [16], neutralization line [17, 18], decoupling network [19, 20], etching slots between antennas [21], hybrid decoupling like ground slit etching and meandered-line parasitic element [22] or slot etching and neutralization line [23], and multimode decoupling technique [24]. Although these isolation techniques, based on additional decoupling structures, provide good isolation enhancement, the antenna efficiency might be reduced significantly. In other words, the isolation improvement is made at the expense of antenna efficiency. For example, the antenna efficiency in [18] and [24] is affected notably, decreasing to 30% and 34%, respectively. Good isolation and antenna performance have been reported by utilizing the self-isolated technique [2, 25]; however, the antenna elements are large and consider a single band MIMO antenna system. In a self-isolated property, an antenna element operates as a radiating element as well as an isolation one at the same time. So, there will be no need for additional decoupling elements or/and isolation techniques. Due to the limited space of mobile terminals, antenna miniaturization is highly requested, and the multi-band is necessary for multiple smartphone applications. Hence, achieving a compact-size multi-band MIMO antenna system with good isolation and radiation efficiency has become a critical challenge.

This paper presents compact, low-profile self-isolated (four and eight elements) antenna arrays operating on triple-bands for 5G MIMO mobile terminals. Based on hybrid fractal geometry, the proposed antenna systems have gained very good antenna miniaturization where the antenna element's overall size is just 11.47 mm × 7.19 mm. In addition, the multi-band and simple structure are presented in the proposed antenna systems where the systems can work in triple resonance frequencies of the n25 band for the extended Personal Communication Systems (PCS) and other related applications, the 5G china mobile band, and the LTE Band-46 band. Due to the antenna element's self-isolated property, good isolation is achieved without inserting any decoupling structures. Furthermore, a high diversity performance with very low envelope correlation coefficients (ECCs) is attained, where excellent independent antenna's far-field radiation characteristics can be shown. Besides, good antenna and MIMO performances are achieved. The proposed antenna systems were simulated and analyzed using the CST Microwave Studio software (version 2019). A prototype model of the proposed eight elements massive MIMO antenna system was fabricated, and its performance was measured. Reasonable agreement between the measured and simulated results has been obtained.

2. THE PROPOSED MIMO ANTENNA SYSTEMS

In this section, the evolution process of the proposed antenna element design will be discussed first. Second, the proposed four-element MIMO antenna system will be presented, including its performance evaluation. Then, the proposed eight-element MIMO antenna system appropriate for the massive 5G mobile phone devices will be introduced and examined. Finally, we will compare the measured and simulated antenna performances of the proposed 8-element MIMO system.

2.1. Evolution of Antenna Element Design

Figure 1(a) depicts the structure and the detailed dimensions of the proposed monopole antenna element. As shown, the antenna element is designed based on a hybrid of modified Minkowski and Peano curves fractal geometries. Very good antenna miniaturization with multi-band capability is obtained by utilizing the space-filling and self-similarity properties of the proposed hybrid fractal geometries where the overall antenna size is (11.47 mm × 7.19 mm). The process of generating the proposed modified Minkowski-Peano antenna element (MMPA) can be shown in Fig. 1(b). The modified Peano curve is superimposed on the modified Minkowski curve achieving a more electrical length with less complexity coming from the higher iterations. Fig. 1(c) demonstrates the generation process of the modified Minkowski curve and modified Peano curve in i and ii, respectively. Since a Minkowski curve and its inverter are joined together to produce the modified Minkowski curve while the modified Peano curve [26] or the generator curve can be created by replacing a straight line (the initiator) with the nine

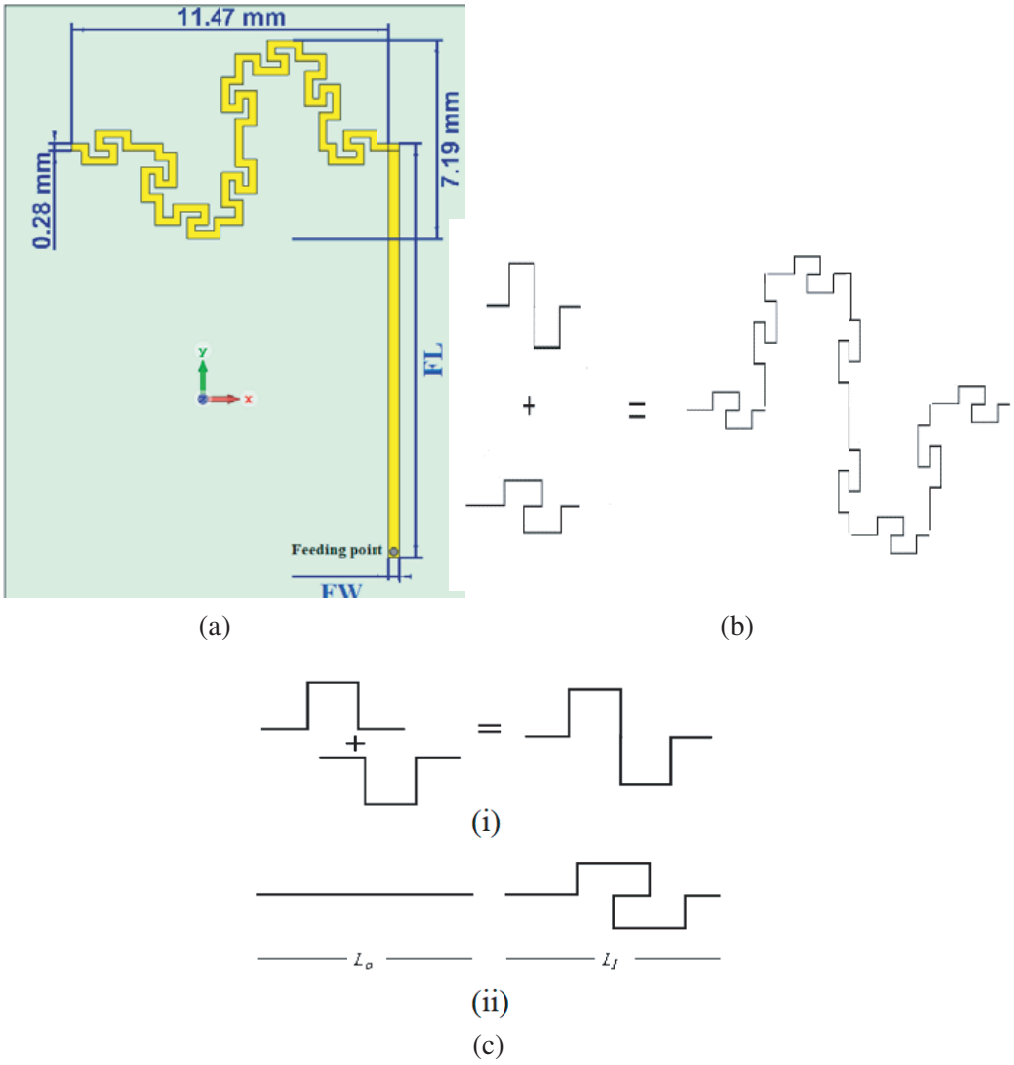

Figure 1. A single antenna. (a) Antenna structure. (b) Generating process of the (MMPA) element. (c) Generating process of the modified Minkowski curve and the modified Peano curve.

segments structure. The proposed antenna generator curve has more segments, which helps fulfil a long electrical antenna length with a small number of iterations. As is depicted, a small length of a 50 Ω transmission line combines with the Minkowski-Peano hybrid curve element for tuning purposes. Each transmission line (TL) is directly fed by a 50 Ω SMA connector via a hole from the proposed system ground's backside.

The effects of FL and FW parameters on the input reflection coefficient have been demonstrated in Figs. 2(a) and (b), respectively. One can see from Fig. 2(a) that four values have been chosen for FL: 11.25 mm, 12.5 mm, 13.75 mm, and 15 mm (the proposed one). As can be observed form Fig. 2(b) that four values have been introduced for the FW parameter which are 0.38 mm (the proposed one), 0.48 mm, 0.58 mm, and 0.78 mm. So the optimized FL parameter value, which is an effective parameter, plays a vital role for obtaining a very good impedance matching. In the next sections, we will discuss the advantages of the proposed antenna structure with its performance in the proposed four and eight MIMO antenna systems.

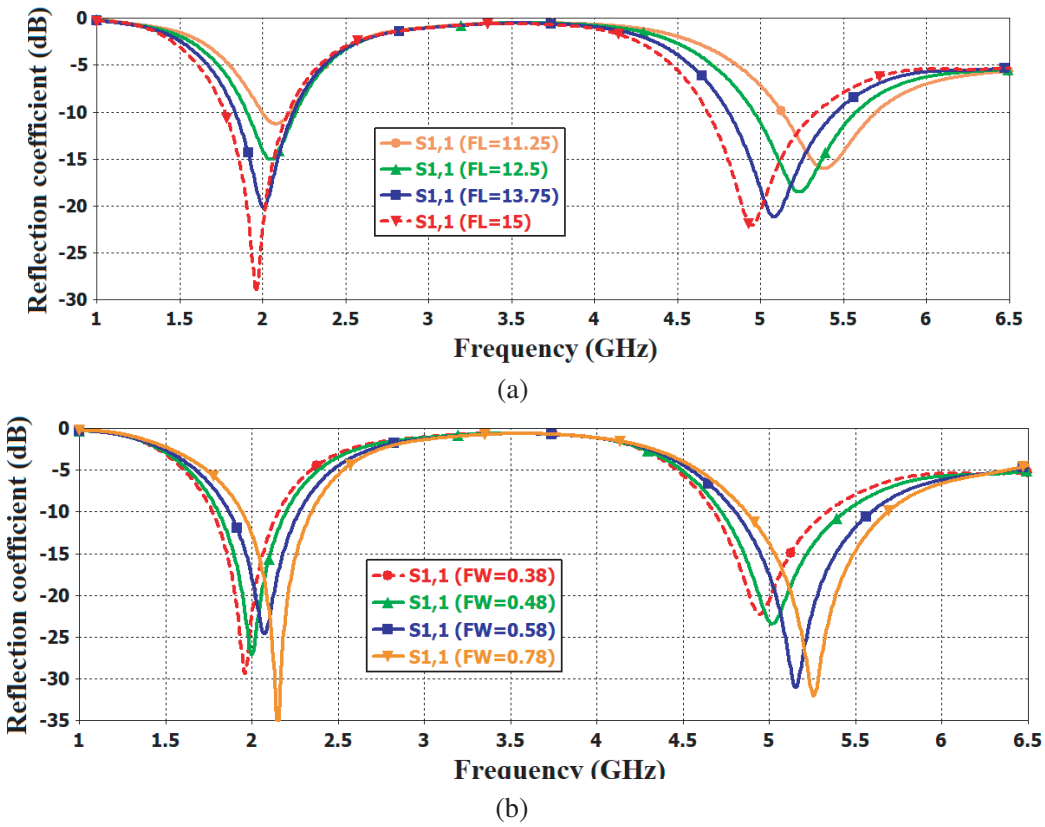

Figure 2. Simulated reflection coefficient. (a) As a function of FL. (b) As a function of FW.

2.2. Proposed Four Elements MIMO Antenna System

The geometry and detailed dimensions of the proposed compact low-profile 4-element MIMO antenna system for the 5G handset applications are shown in Fig. 3. As observed in Fig. 3(a), all four antennas are printed on the surface layer of a system substrate. They are located at the mobile board's corners and symbolized as Ant1, Ant2, Ant3, and Ant4. The optimal location and orientation of the antenna elements at the top four corners of the mobile device have been chosen to utilize the mobile's space as much as possible and obtain a better performance. The proposed antenna system is designed by employing a double-sided FR4 substrate of 0.8 mm height, which has a relative permittivity of 4.3 and a loss tangent of 0.02. The main system board size is $(150 \times 75)\,\text{mm}^2$. It is a typical size of 5.5-inch handset. Fig. 3(b) illustrates the system ground bottom layer, which is defected to improve the antenna bandwidth and matching. All the proposed MIMO antenna elements have the same structure and dimensions.

Figure 4 depicts the simulated S-parameters results of the proposed compact low-profile four antenna elements MIMO system. From Fig. 4(a), the accepted impedance matching of less than -6 dB (3 : 1 VSWR) is obtained over the desired operation bands. This proposed system works at two dual-wideband of (1.66–2.30) GHz and (4.55–5.93) GHz with triple resonance frequencies that cover (1.661–2.305) GHz for the extended Personal Communication Purposes (PCS) n25 and other related applications, the china band (4.8–5) GHz, and the LTE Band-46 (5.150–5.925) GHz. As shown in Fig. 4(b), good isolation is achieved (better than 12.4 dB in the lower band and 14.8 dB in the higher operating bands) without employing any decoupling elements and/or isolation techniques.

As depicted in Fig. 5, desirable total and radiation antenna efficiencies for all four antennas of the proposed MIMO system are obtained. The total antenna efficiencies of the triple (1.661–2.305) GHz, (4.8–5) GHz, and (5.150–5.925) GHz working bands are (57–60)%, (78–83)%, and (60–82)% GHz, respectively, while the radiation antenna efficiencies are (88–89)%, (86–87)%, and (88–83)%,

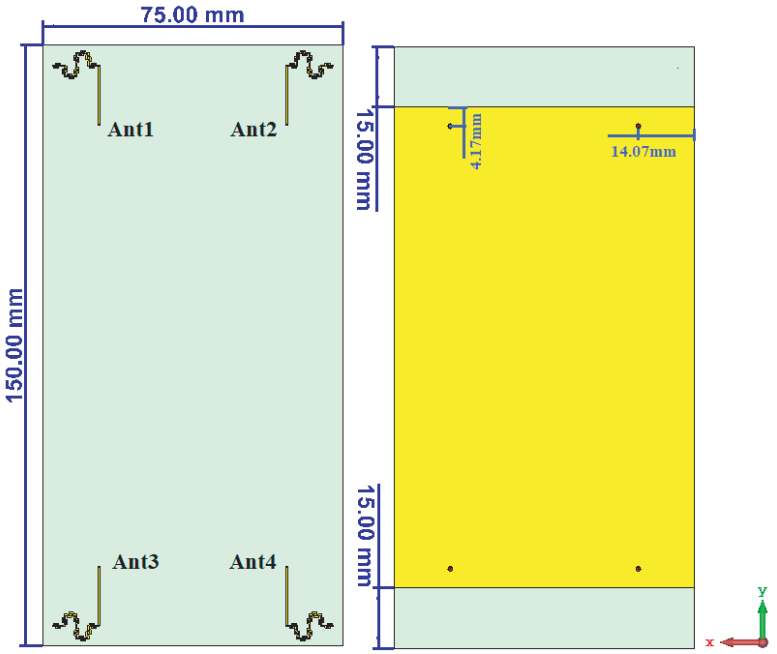

Figure 3. The proposed four-element MIMO antenna system. (a) Top-side view. (b) Backside view.

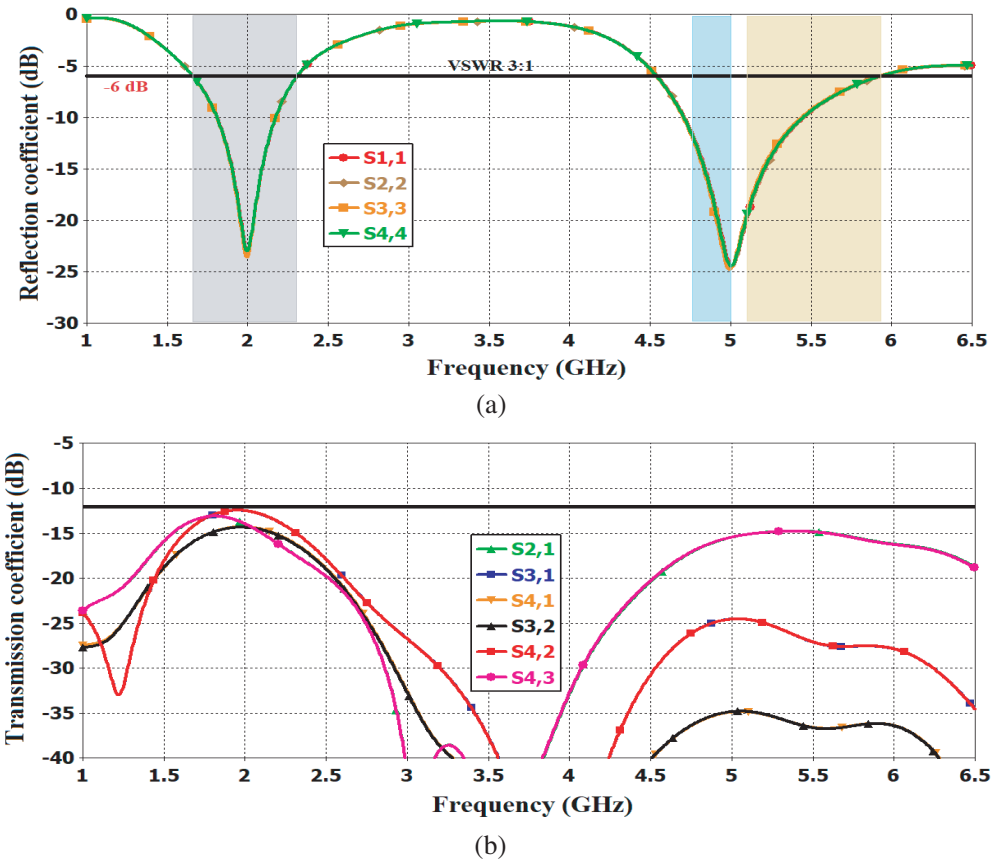

Figure 4. *S*-parameters. (a) Reflection coefficients. (b) Transmitting coefficients.

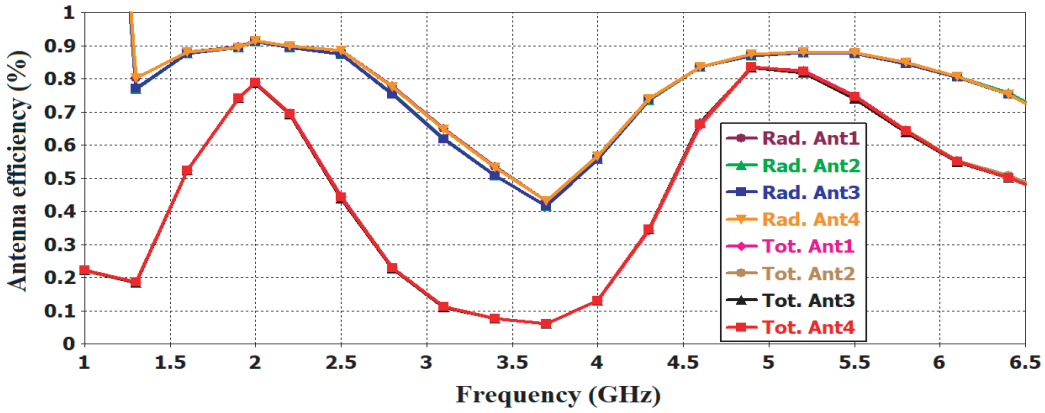

Figure 5. Antenna efficiency.

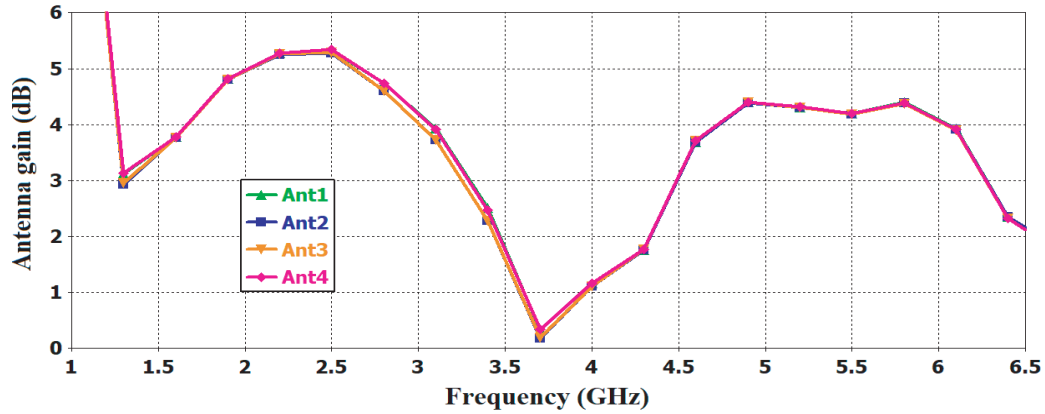

Figure 6. Antenna gain.

respectively. The four antennas' gain along the bands of interest are exhibited in Fig. 6. As it is seen, the gains are almost stable within the operating bands, and high gains of all antennas are attained where the maximum gains are about 5.3 dB, 4.4 dB, and 4.3 dB for the (1.661–2.305) GHz, (4.8–5) GHz, and (5.150–5.925) GHz interested bands, respectively.

2.3. Proposed Eight Elements MIMO Antenna System

The structure with the detailed dimensions of the proposed compact self-isolated eight-element MIMO antenna system for the 5G smartphone devices is depicted in Fig. 7. The proposed antenna main system board (including the dimensions and substrate specifications) is the same as that employed in Fig. 3 for the four-element MIMO antenna system, except that eight antenna elements (instead of four) are placed on the surface layer of the system substrate. As shown in Fig. 7(a), the four antennas located at the mobile phone's corners are symbolized as Ant1, Ant2, Ant3, and Ant4, while the four antennas located at the middle of the mobile phone are denoted by Ant5, Ant6, Ant7, and Ant8. As observed in Fig. 7(b), the system ground bottom layer is defected in the same manner as the proposed four elements MIMO system for improving antenna bandwidth and matching purposes. All the eight antenna elements have the same structure and dimensions, appropriate for 5G massive MIMO antenna systems with slim smartphone requirements.

The simulated results of the S-parameters for the proposed eight elements MIMO antenna system are plotted in Fig. 8. As depicted in Fig. 8(a), all the eight reflection coefficients of the antennas satisfy values less than -6 dB (3 : 1 VSWR) over all the bands of interest, which ensures an accepted

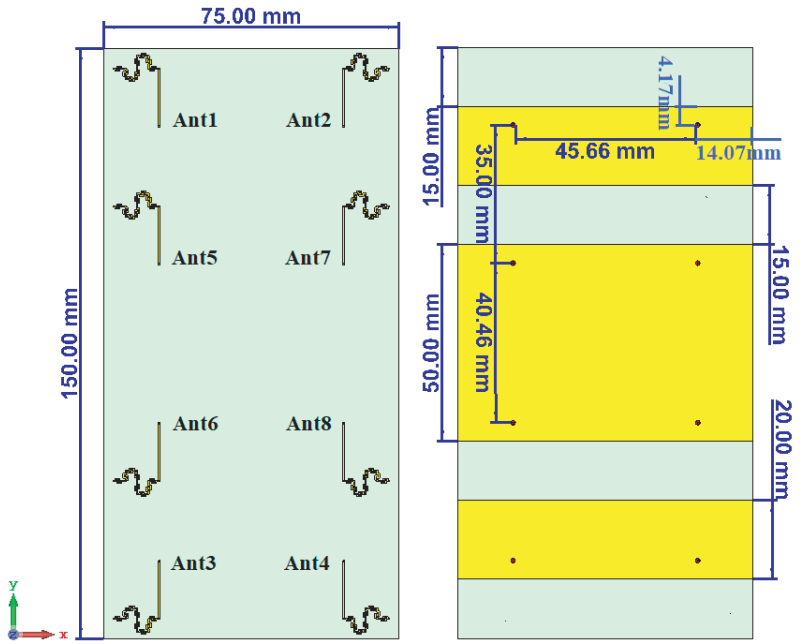

(a) (b)

Figure 7. The proposed eight-element MIMO antenna system. (a) Top-side view. (b) Backside view.

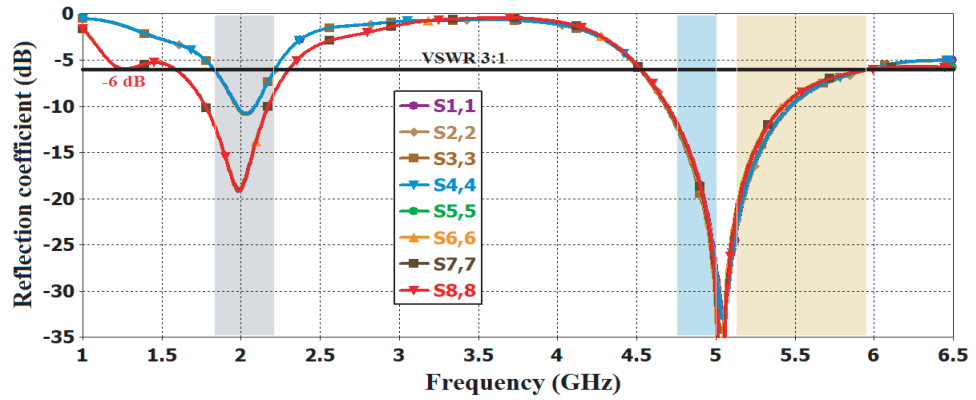

(a)

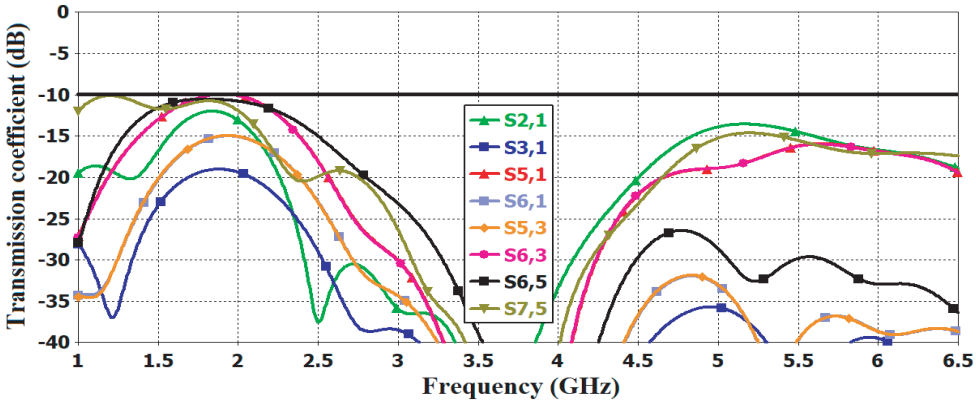

(b)

Figure 8. *S*-parameters. (a) Reflection coefficients. (b) Transmitting coefficients.

impedance matching of the proposed system. The proposed eight elements MIMO antenna system can work on triple bands of (1.83–2.21) GHz for the extended Personal Communication Purposes (PCS) n25 and other related applications, the china band (4.8–5) GHz, and the LTE Band-46 (5.150–5.925) GHz. From Fig. 8(b), good isolation is attained without utilizing any additional isolation structures and/or decoupling methods. The transmission coefficients S_{21}, S_{51}, S_{63}, S_{65}, S_{75} are better than 10 dB, while S_{31}, S_{61}, S_{53} are almost better than 15 dB within the lower band (1.83–2.21) GHz. In the higher bands of (4.8–5) GHz and (5.150–5.925) GHz, the transmission coefficients S_{21}, S_{51}, S_{63}, S_{75} are better than 13.5 dB, whereas S_{31}, S_{61}, S_{53}, S_{65} are better than 26.5 dB. The desirable impedance matching and isolation are achieved without using matching circuits, re-optimizing the antenna structure, additional isolation elements, and/or other decoupling methods that increase system complexity and reduce antenna efficiency. So, this indicates the ability of the proposed self-isolated antenna structure to work well at different array elements. This is one of the advantages of the proposed antenna system.

The maximum gain within the (1.83-2.21) GHz band of the four antennas located at the top four corners of the mobile mainboard (Ant1, Ant2, Ant3, and Ant4) is 2.7 dB. For the other four antennas, placed in the middle of the mobile board (Ant5, Ant6, Ant7, and Ant8), the maximum gain is 2 dB."

The total and radiation antenna efficiencies of the proposed MIMO systems' eight antennas are sketched in Fig. 9. Desirable antenna efficiencies are attained where the total antenna efficiencies of the triple operating bands (1.83–2.21) GHz, (4.8–5) GHz, and (5.150–5.925) GHz are (46–56)%, (81–82)%, and (57–80)% GHz, respectively, whereas the radiation antenna efficiencies are (77–89)%, (86–87)%, and (80–87)%, respectively. Fig. 10 shows the eight antennas' gain of the proposed antenna system along the working bands. As illustrated, good antennas' gains are obtained, appropriate for mobile terminals' 5G antenna requirement. The maximum gain within the (1.83–2.21) GHz band of the four antennas

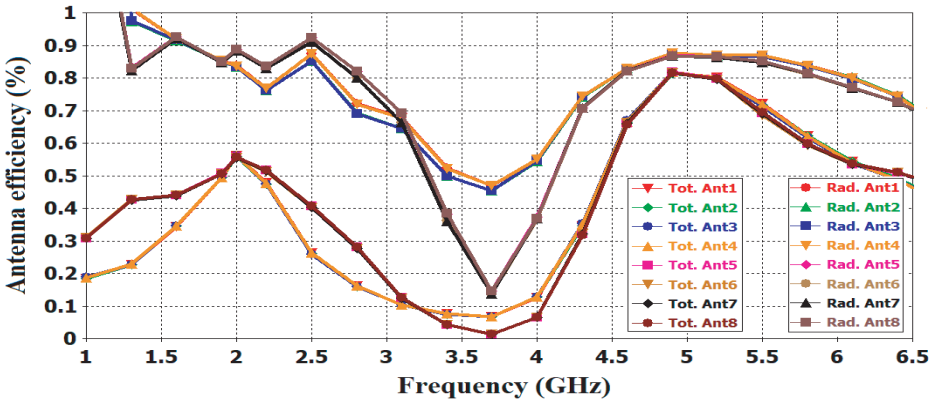

Figure 9. Antenna efficiency.

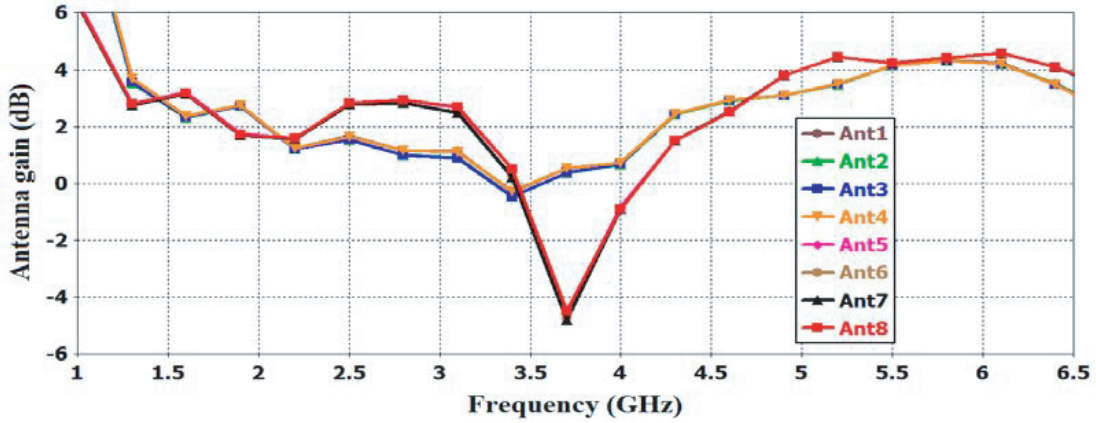

Figure 10. Antenna gain.

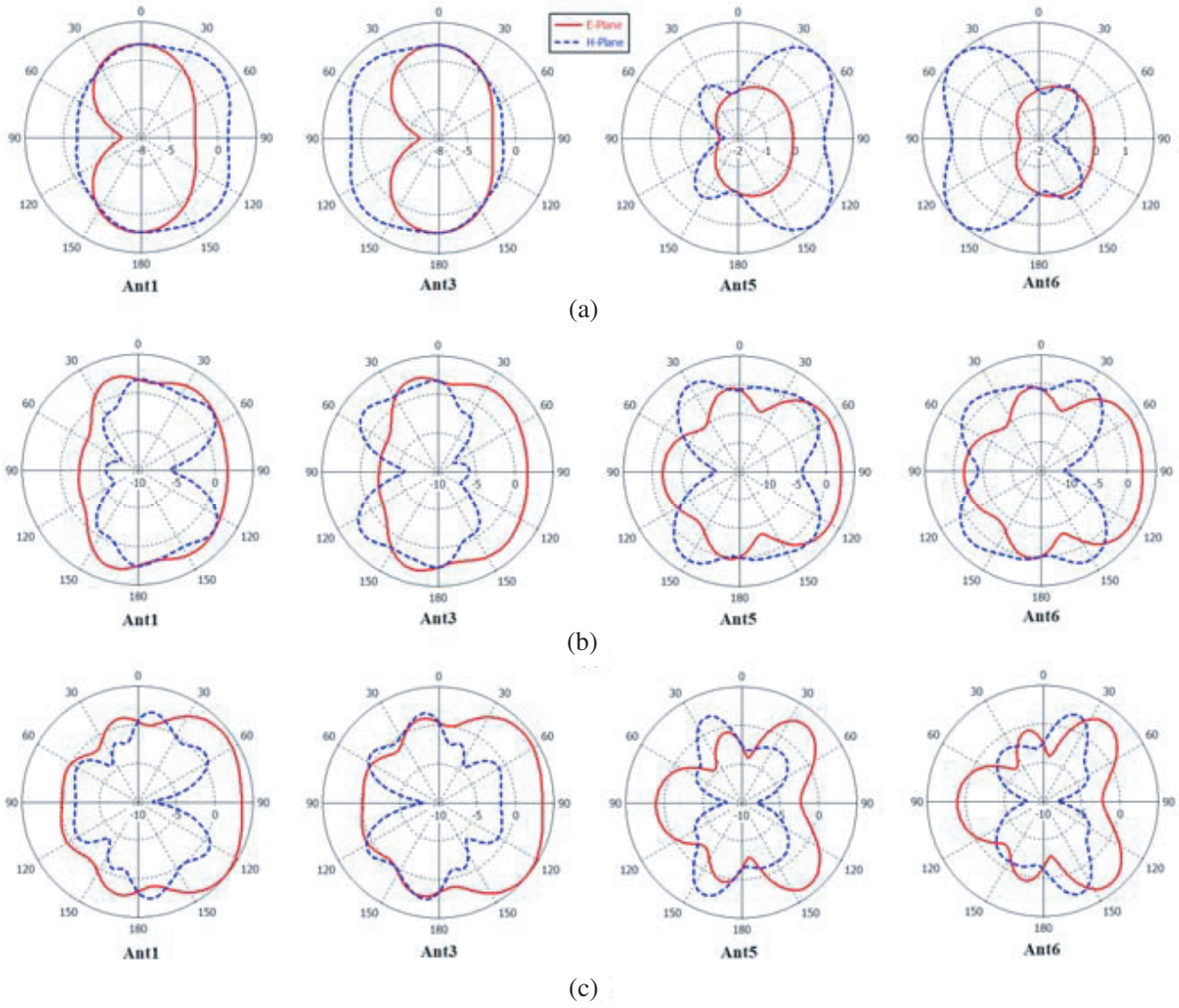

Figure 11. The two dimensional-antenna radiation patterns (a) at 2 GHz, (b) at 4.9 GHz, (c) at 5.5 GHz.

located at the top four corners of the mobile mainboard (Ant1, Ant2, Ant3, and Ant4) is 2.7 dB. For the other four antennas, placed in the middle of the mobile board (Ant5, Ant6, Ant7, and Ant8), the maximum gain is 2 dB. Concerning the (4.8–5) GHz band, the maximum gain of the top four corners and middle antennas are 3.2 dB and 4 dB, respectively, whereas the (5.150–5.925) GHz bands are 4.3 dB and 4.4 dB, respectively. Because of the similarity and brevity, the two-dimensional radiation patterns at the triple operating bands of one-sided antennas (Ant1, Ant3, Ant5, and Ant6) are exhibited in Fig. 11. In contrast, the three-dimensional radiation patterns are displayed in Fig. 12. As observed, each antenna element has a maximum gain direction different from other antennas' maximum gain directions, indicating a magnificent pattern diversity feature of the proposed 8-element MIMO antenna system. Moreover, all sides of the mobile device board are entirely covered by these eight antennas' radiation patterns. So, an eligible radiation coverage performance is obtained by the proposed MIMO antenna system.

The Envelope Correlation Coefficients (ECCs) and Mean effective gains (MEGs) are calculated and analyzed to assess the MIMO performance of the proposed eight elements antenna array. The correlation coefficient (ρ) indicates how much the multipath communication channels are correlated or

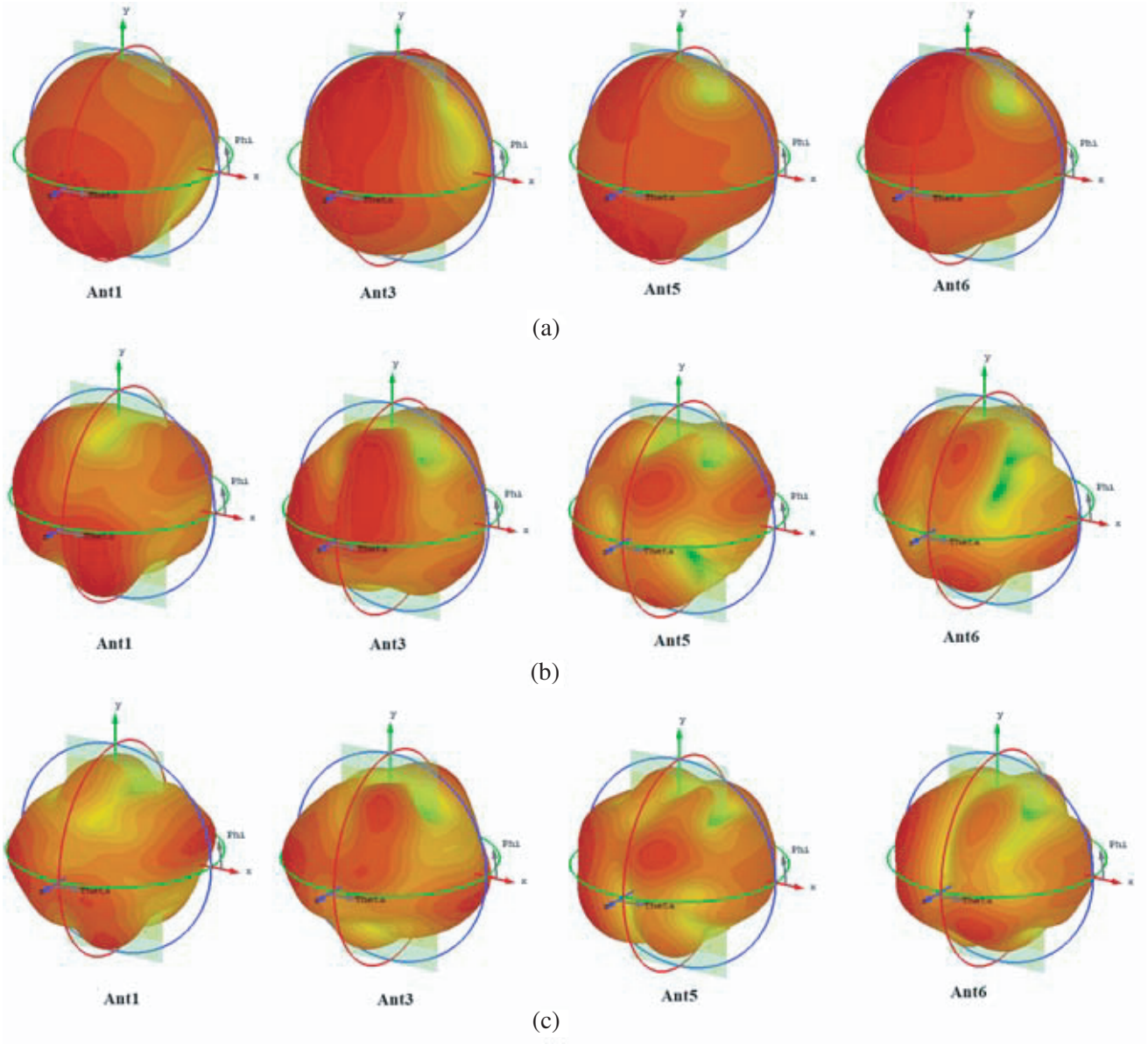

Figure 12. The three-dimensional antenna radiation patterns (a) at 2 GHz, (b) at 4.9 GHz, (c) at 5.5 GHz.

isolated (i.e., a measure of the independency) [27]. This metric refers to the correlation between the antenna radiation patterns. The square of the correlation coefficient (ρ^2) is defined as the Envelope Correlation Coefficient (ρ_e). The ECC can be calculated based on the far-field radiation patterns using Equation (1) [28]:

$$\rho_e = \frac{\left| \iint_{4\pi} \left[\vec{F}_1(\theta,\varphi) * \vec{F}_2(\theta,\varphi) \right] d\Omega \right|^2}{\iint_{4\pi} \left| \vec{F}_1(\theta,\varphi) \right|^2 d\Omega \iint_{4\pi} \left| \vec{F}_2(\theta,\varphi) \right|^2 d\Omega} \tag{1}$$

where Ω defines the solid angle; $(\vec{F}_i(\theta,\varphi))$ indicates the three-dimensional far-field radiation pattern; and the asterisk sign $(*)$ refers to the Hermitian product. In addition to that, the ECC can be obtained

simply in terms of the S-parameters from Equation (2) as indicated in [29]:

$$|\rho_e(i,j,N)| = \frac{\left|\sum_{n=1}^{N} S_{i,n}^{*} S_{n,j}\right|}{\sqrt{\left|\prod_{k(=i,j)}\left[1-\sum_{n=1}^{N} S_{i,n}^{*} S_{n,k}\right]\right|}} \tag{2}$$

In this formula, N is the number of antennas, and the antenna elements are expressed as i and j, respectively. For acceptable MIMO performance, the values of ECCs between the MIMO antennas should be less than 0.5. The smaller the ECCs are, the better the MIMO system diversity performance is [30]. The ECCs between the antennas in the proposed eight elements MIMO system are plotted in Fig. 13, calculated based on the E-filed radiation patterns of Equation (1) under the hypothesis of uniform propagation channel with balanced polarization. As observed, the ECCs are less than 0.195, 0.005, and 0.022 for the (1.83–2.21) GHz, (4.8–5) GHz, and (5.150–5.925) GHz bands of interest, respectively. They are far less from the accepted criteria of ECC < 0.5. So the proposed MIMO antenna system has a capability of a high diversity performance.

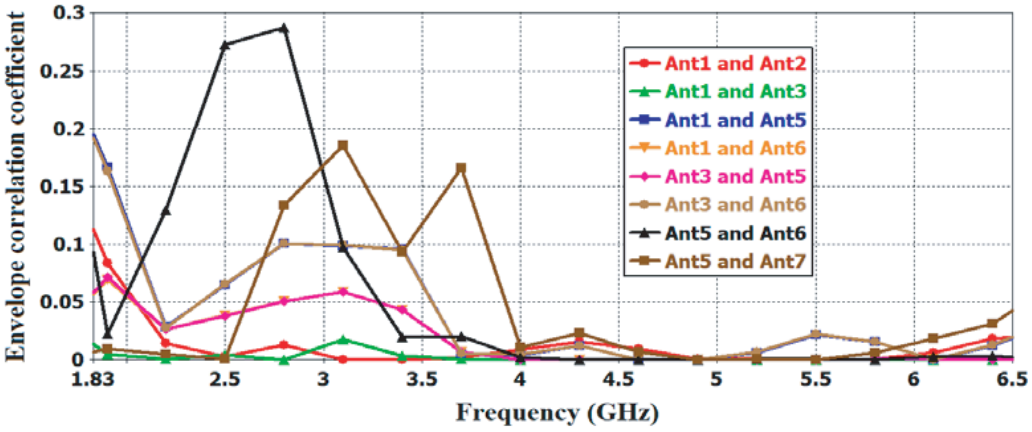

Figure 13. ECCs of the proposed system.

The MEG metric can be recognized as the ratio of the antenna's mean received power to the total mean incident power when the antenna is moved over a random mobile environment route. A MEG can be obtained from Equation (3) [31]:

$$MEG = \int_0^{2\pi}\int_0^{\pi}\left(\frac{XPR}{1+XPR}G_\theta(\theta,\varphi)P_\theta(\theta,\varphi) + \frac{1}{1+XPR}G_\varphi(\theta,\varphi)P_\varphi(\theta,\varphi)\right)(\sin\theta)d\theta d\varphi \tag{3}$$

where the cross-polarization power ratio is denoted as XPR, and P_φ and P_θ indicate the phi and theta components of the normalized angular power density functions of the incoming plane waves, while G_θ and G_φ are the antenna gain components. It is worth noting that for good MIMO antenna system diversity performance and system power balance, the MEGs of the MIMO antennas should satisfy the required criteria of ($MEG_i \cong MEG_j$) [13], where MEG_i and MEG_j are the mean effective gains of the i and j antennas, respectively. Fig. 14 depicts the MEGs for all eight antennas of the proposed MIMO system, which are taken under the assumption of uniform distribution for the azimuth direction and Gaussian distribution for the elevation direction of the angular power density function. It can be seen that the MEGs for all antennas are stable along the triple operating bands. Furthermore, the MEGs nearly satisfy the equality condition of the antenna elements in the designed MIMO system.

The proposed 8-element MIMO smartphone antenna was fabricated and experimentally tested. The fabricated prototype model is demonstrated in Fig. 15. Through the measurement process, each

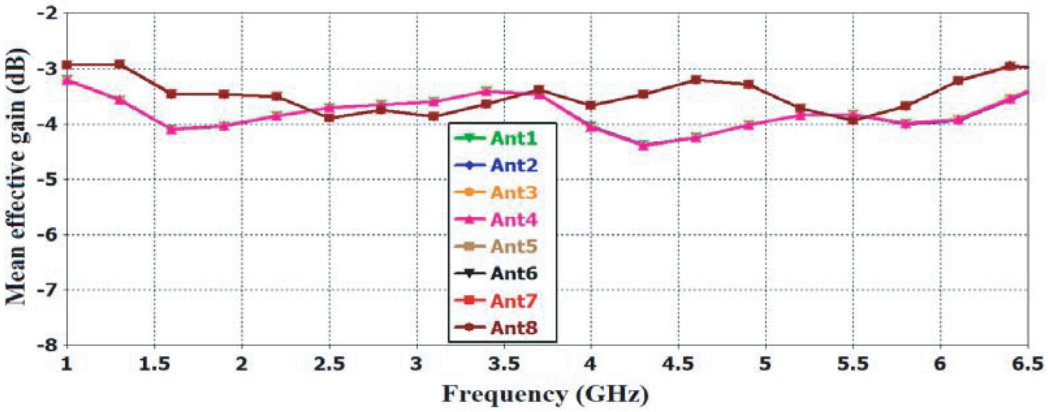

Figure 14. MEGs of the proposed eight antennas.

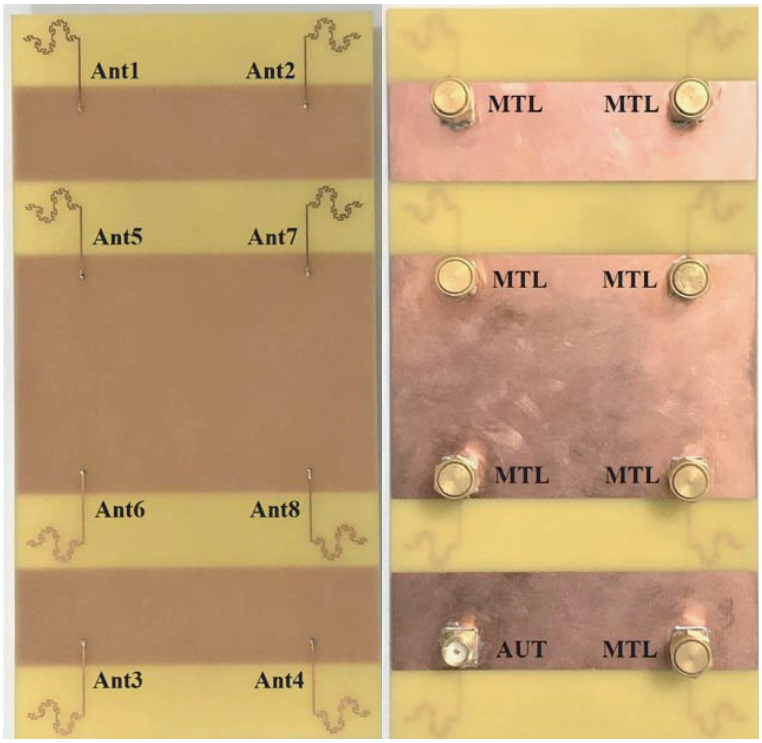

(a) (b)

Figure 15. Fabricated prototype model of the proposed eight elements MIMO antenna system. (a) Top-side view. (b) Backside view.

antenna under test (AUT) is connected to the vector network analyzer (VNA), and other antenna elements are connected to 50 Ω matched terminal loads (MTLs). Due to the similarity and brevity, only the necessary simulated and measured S-parameters have been plotted in Figs. 16(a) and (b), respectively. As observed, desirable impedance matching and isolation performance (better than 11 dB in the lower band and 17 dB in the higher operating bands) are obtained by the proposed MIMO antenna system. The measured and simulated results are in good agreement. However, some deviations between them may be due to fabrication tolerances, soldering effects, and/or measurement errors.

Table 1 presents a summary for the performance comparison of the proposed four and eight elements

Table 1. A comparison with other recent works.

Ref.	Bandwidth (GHz)	Total efficiency (%)	Isolation (dB)	Mainboard mobile size (mm^2)	Antenna element Size (mm × mm)	MIMO order	Isolation technique
[32]	(3.4–3.6) (4.8–5.0)	> 50	> 17.5	(75 × 150)	(22 × 7)	4 × 4	Self-isolated
[33]	(3.3–4.2)	> 40	> 10	(70 × 150)	(42 × 42)	4 × 4	Self-isolated
[34]	(3.3–4.2)	> 61	> 17.9	(75 × 150)	(26 × 6.2)	4 × 4	Self-isolated
[35]	(3.3–5)	> 46	> 14.5	(75 × 150)	(22 × 6)	8 × 8	Self-isolated
[36]	(2.55–2.65)	(48–58)	> 13	(68 × 136)	(18.6 × 18.6)	8 × 8	Polarization diversity
[37]	(3.3–3.6)	(42–75)	> 13	(75 × 155)	(28.8 × 1)	8 × 8	Balanced mode excitation
[38]	2.55–2.65	(48–63)	> 12.5	(68 × 136)	(31.2 × 5)	8 × 8	Polarization diversity and Pattern diversity
[17]	(3.4–3.6) (4.8–5.1)	(41–72) (40–85)	> 11.5	(75 × 150)	(15 × 7)	8 × 8	Neutralization line
[39]	(3.4–3.6) (5.15–5.925)	(51–59) (62–80)	> 11.2	(70 × 140)	16.3 × 10	8 × 8	Self-isolated
[31]	(1.88–1.92) (2.3–2.62)	(40–55) (50–70)	> 10	(68.8 × 136)	14 × 15	8 × 8	Pattern diversity
This work	(1.66–2.30) (4.8–5) (5.150–5.925)	(57–60) (78–83) (60–82)	> 12.4 > 14.8 > 14.8	(75 × 150)	11.47 × 7.19	4 × 4	Self-isolated
	(1.83–2.21) (4.8–5) (5.150–5.925)	(46–56) (81–82) (57–80)	> 11 > 17 > 17	(75 × 150)	11.47 × 7.19	8 × 8	Self-isolated

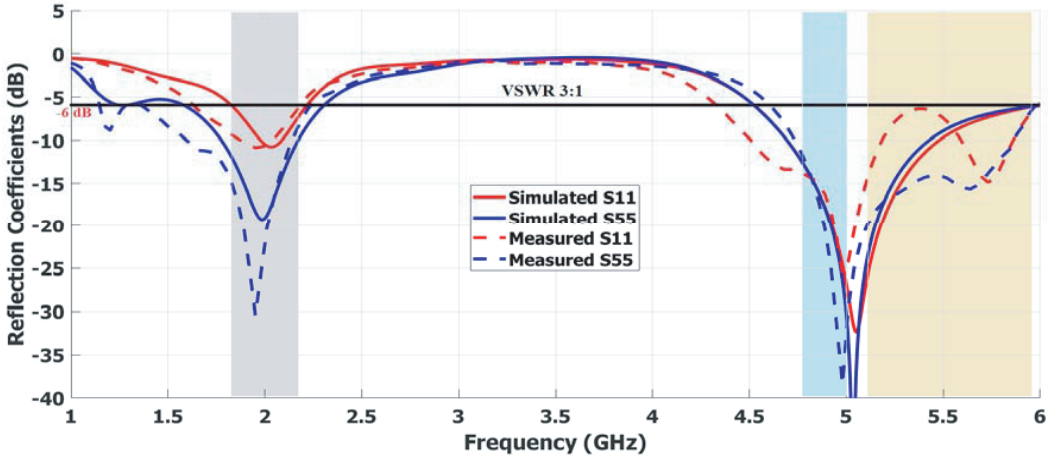

(a)

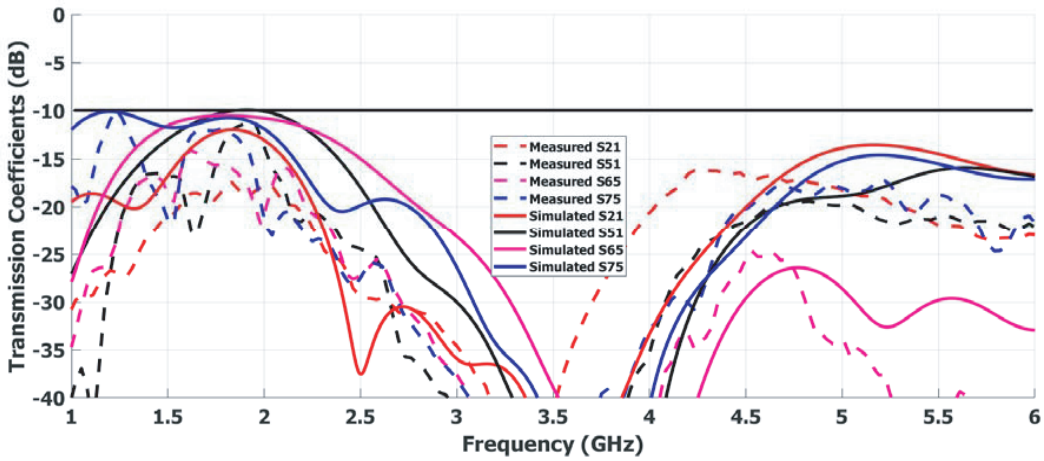

(b)

Figure 16. Measured and simulated S-parameters. (a) Reflection coefficients. (b) Transmission coefficients.

MIMO antenna systems with some other recent MIMO antenna systems reported for the 5G mobile phone devices. Compared with other MIMO antenna systems, we suggested a triple-band and smaller size design of low-profile four and eight elements MIMO antenna systems. Good system isolation and antenna total efficiencies are obtained by adopting the self-isolation property where there is no additional antenna efficiency loss by other decoupling elements and/or isolation techniques. So it can be seen from Table 1 that the proposed antenna systems are able to provide MIMO systems with very comparable antenna and MIMO performances.

3. CONCLUSIONS

In this study, compact four and eight elements MIMO antenna systems are introduced and examined for 5G mobile phone devices. Very good antenna miniaturization is achieved by utilizing the Minkowski-Peano hybrid curve fractal geometry's space-filling property. Due to the self-isolated property, good isolation is achieved without adopting any matching circuits, isolation elements, decoupling methods, and/or re-optimizing the antenna structure, increasing system complexity and reducing antenna efficiency. This indicates the proposed self-isolated antenna structure's ability to work well at different array elements. The Minkowski-Peano hybrid curve fractal geometry shows a good ability to achieve the antenna elements with the self-isolated property and multi-band resonance frequency. The performance of the proposed MIMO antenna systems indicates that these systems will be a convincing candidate for the 5G smartphone terminals.

REFERENCES

1. Han, C. Z., L. Xiao, Z. Chen, and T. Yuan, "Co-located self-neutralized handset antenna pairs with complementary radiation patterns for 5G MIMO applications," *IEEE Access*, Vol. 8, 73151–73163, 2020.
2. Zhao, A. and Z. Ren, "Size reduction of self-isolated MIMO antenna system for 5G mobile phone applications," *IEEE Antennas and Wireless Propagation Letters*, Vol. 18, No. 1, 152–156, 2019.
3. Varzakas, P., "Average channel capacity for Rayleigh fading spread spectrum MIMO systems," *International Journal of Communication Systems*, Vol. 19, No. 10, 1081–1087, 2006.
4. Varzakas, P., "Estimation of optimum antennas number of a spread spectrum MIMO system under signal fading," *WSEAS Transactions on Computers*, Vol. 18, 281–284, 2019.

5. Varzakas, P., "Closed-form expression for the optimum antennas number of a spread spectrum MIMO system under Rayleigh fading conditions," *Proceedings of the 13th WSEAS International Conference on Communications*, 56–59, Rodos, Greece, 2009.
6. Muhsin, M. Y., A. J. Salim, and J. K. Ali, "A compact self-isolated MIMO antenna system for 5G mobile terminals," *Computer Systems Science and Engineering*, Vol. 42, No. 3, 919–934, 2022.
7. Salim, A. J., R. S. Fyath, A. H. Ahmed, and J. K. Ali, "A new fractal based PIFA antenna design for MIMO dual band WLAN applications," *PIERS Proceedings*, 1526–1530, Kuala Lumpur, Malaysia, 2012.
8. Zou, H., Y. Li, H. Shen, H. Wang, and G. Yang, "Design of 6×6 dualband MIMO antenna array for 4.5G/5G smartphone applications," *Sixth Asia-Pacific Conference on Antennas and Propagation (APCAP)*, 1–3, Xi'an, China, 2017.
9. Salim, A. J., R. S. Fyath, and J. K. Ali, "A new miniaturized folded fractal based PIFA antenna design for MIMO wireless applications," *Proceedings of the International Conference on Information and Communication Technology*, 36–40, Baghdad, Iraq, 2019.
10. Li, Y., C. Sim, Y. Luo, and G. Yang, "High-isolation 3.5 GHz eight-antenna MIMO array using balanced open-slot antenna element for 5G smartphones," *IEEE Transactions on Antennas and Propagation*, Vol. 67, No. 6, 3820–3830, 2019.
11. Li, M., Y. Ban, Z. Xu, J. Guo, and Z. Yu, "Tri-polarized 12-antenna MIMO array for future 5G smartphone applications," *IEEE Access*, Vol. 6, 6160–6170, 2018.
12. Ding, C. F., X. Y. Zhang, C. D. Xue, and C. Y. D. Sim, "Novel pattern-diversity-based decoupling method and its application to multi-element MIMO antenna," *IEEE Transactions on Antennas and Propagation*, Vol. 66, No. 10, 4976–4985, 2018.
13. Abdullah, M., S. H. Kiani, and A. Iqbal, "Eight element Multiple-Input Multiple-Output (MIMO) antenna for 5G mobile applications," *IEEE Access*, Vol. 7, 134488–134495, 2019.
14. Jiang, W., Y. Cui, B. Liu, W. Hu, and Y. Xi, "A dual-band MIMO antenna with enhanced isolation for 5G smartphone applications," *IEEE Access*, Vol. 7, 112554–112563, 2019.
15. Parchin, N., Y. AL-Yasir, A. Ali, I. Elfergani, J. Noras, et al., "Eight-element dual-polarized MIMO slot antenna system for 5G smartphone applications," *IEEE Access*, Vol. 7, 15612–15622, 2019.
16. Hu, W., X. Liu, S. Gao, L. Wen, L. Qian, et al., "Dual-band ten-element MIMO array based on dual-mode IFAs for 5G terminal applications," *IEEE Access*, Vol. 7, 178476–178485, 2019.
17. Guo, J., L. Cui, C. Li, and B. Sun, "Side-edge frame printed eight-port dual-band antenna array for 5G smartphone applications," *IEEE Transactions on Antennas and Propagation*, Vol. 66, No. 12, 7412–7417, 2018.
18. Wong, K., J. Lu, L. Chen, W. Li, and Y. Ban, "8-antenna and 16-antenna arrays using the quad-antenna linear array as a building block for the 3.5-GHz LTE MIMO operation in the smartphone," *Microwave and Optical Technology Letters*, Vol. 58, No. 1, 174–181, 2016.
19. Qian, K. and D. Gan, "Compact tunable network for closely spaced antennas with high isolation," *Microwave and Optical Technology Letters*, Vol. 58, No. 1, 65–69, 2016.
20. Baek, J. and J. Choi, "The design of a LTE/MIMO antenna with high isolation using a decoupling network," *Microwave and Optical Technology Letters*, Vol. 56, No. 9, 2187–2191, 2014.
21. Hu, W., L. Qian, S. Gao, L. Wen, Q. Luo, et al., "Dual-band eight-element MIMO array using multi-slot decoupling technique for 5G terminals," *IEEE Access*, Vol. 7, 153910–153920, 2019.
22. Deng, J., J. Li, L. Zhao, and L. Guo, "A dual-band inverted-F MIMO antenna with enhanced isolation for WLAN applications," *IEEE Antennas and Wireless Propagation Letters*, Vol. 16, 2270–2273, 2017.
23. Jiang, W., B. Liu, Y. Cui, and W. Hu, "High-isolation eight-element MIMO array for 5G smartphone applications," *IEEE Access*, Vol. 7, 34104–34112, 2019.
24. Xu, H., H. Zhou, S. Gao, H. Wang, and Y. Cheng, "Multimode decoupling technique with independent tuning characteristic for mobile terminals," *IEEE Transactions on Antennas and Propagation*, Vol. 65, No. 12, 6739–6751, 2017.

25. Zhao, A. and Z. Ren, "Multiple-input and multiple-output antenna system with self-isolated antenna element for fifth-generation mobile terminals," *Microwave and Optical Technology Letters*, Vol. 61, No. 1, 20–27, 2019.
26. Salim, A. J. and J. K. Ali, "Design of internal dual band printed monopole antenna based on Peano-type fractal geometry for WLAN USB dongle," *PIERS Proceedings*, 1268–1272, Suzhou, China, 2011.
27. Aziz, H. and D. Naji, "Compact dual-band MIMO antenna system for LTE smartphone applications," *Progress In Electromagnetics Research C*, Vol. 102, 13–30, 2020.
28. Cai, Q., Y. Li, X. Zhang, and W. Shen, "Wideband MIMO antenna array covering 3.3–7.1 GHz for 5G metal-rimmed smartphone applications," *IEEE Access*, Vol. 7, 142070–142084, 2019.
29. Blanch, S., J. Romeu, and I. Corbella, "Exact representation of antenna system diversity performance from input parameter description," *Electronics Letters*, Vol. 39, No. 9, 705–707, 2003.
30. Muhsin, M. Y., A. J. Salim, and J. K. Ali, "An eight-element MIMO antenna system for 5G mobile handsets," *International Symposium on Networks, Computers and Communications (ISNCC)*, 1–4, Dubai, United Arab Emirates, 2021.
31. Qin, Z., W. Geyi, M. Zhang, and J. Wang, "Printed eight-element MIMO system for compact and thin 5G mobile handest," *Electronics Letters*, Vol. 52, No. 6, 416–418, 2016.
32. Ren, Z. and A. Zhao, "Dual-band MIMO antenna with compact self-decoupled antenna pairs for 5G mobile applications," *IEEE Access*, Vol. 7, 82288–82296, 2019.
33. Barani, I., K. Wong, Y. Zhang, and W. Li, "Low-profile wideband conjoined open-slot antennas fed by grounded coplanar waveguides for 4×4 5G MIMO operation," *IEEE Transactions on Antennas and Propagation*, Vol. 68, No. 4, 2646–2657, 2020.
34. Zhao, A. and Z. Ren, "5G MIMO antenna system for mobile terminals," *IEEE International Symposium on Antennas and Propagation and USNC-URSI Radio Science Meeting*, 427–428, Atlanta, USA, 2019.
35. Zhao, A. and Z. Ren, "Wideband MIMO antenna systems based on coupled-loop antenna for 5G N77/N78/N79 applications in mobile terminals," *IEEE Access*, Vol. 7, 93761–93771, 2019.
36. Li, M., Z. Xu, Y. Ban, C. Sim, and Z. Yu, "Eight-port orthogonally dual-polarized MIMO antennas using loop structures for 5G smartphone," *IET Microwaves, Antennas & Propagation*, Vol. 11, No. 12, 1810–1816, 2017.
37. Huang, D., Z. Du, and Y. Wang, "Slot antenna array for fifth generation metal frame mobile phone applications," *Int. Journal of RF and Microwave Computer-Aided Engineering*, Vol. 29, No. 9, 1–9, 2019.
38. Li, M., Y. Ban, Z. Xu, G. Wu, C. Sim, et al., "Eight-port orthogonally dual-polarized antenna array for 5G smartphone applications," *IEEE Transactions on Antennas and Propagation*, Vol. 64, No. 9, 3820–3830, 2016.
39. Li, J., X. Zhang, Z. Wang, X. Chen, J. Chen, Y. Li, and A. Zhang, "Dual-band eight-antenna array design for MIMO applications in 5G mobile terminals," *IEEE Access*, Vol. 7, 71636–71644, 2019.